Design and Performance Assessment of a Mini Underwater Robot

Rafiuddin Syam [1,*], Azwar Hayat [2], Syaiful Bakhri [3], Andi Amijoyo Mochtar [2], and Hamdani [2]

[1] Automation Eng. Technology Dept., Faculty of Engineering, Universitas Negeri Jakarta, Jakarta, Indonesia
[2] Mechanical Engineering Department, Hasanuddin University, Makassar, Indonesia
3 National Nuclear Energy Agency of Indonesia, BATAN, Banten, Indonesia
Email: rafiuddin_syam @unj.ac.id (R.S.); azwar.hayat@unhas.ac.id (A.H.); syaiful.bakhri@batan.go.id (S.B.); andijoyo@unhas.ac.id (A.A.M.); hamdanirobot@gmail.com (H.)
*Corresponding author

***Abstract*—This paper presents the design, implementation, and performance evaluation of a miniature underwater Remotely Operated Vehicle (ROV) specifically developed for leak detection in industrial tanks and reactors. The compact robot (390 × 85 × 85 mm) features a lightweight Polylactic Acid (PLA) frame and is powered by a LiPo battery, achieving optimal balance between structural integrity and maneuverability. The system incorporates a quad-propeller configuration, four 60-mm-diameter propellers with three CW/CCW blades each, and a front-mounted camera for navigation and inspection. Controlled via a wired connection providing both power and telemetry, the ROV demonstrates exceptional motion stability—a critical factor for reliable leak detection in confined underwater environments. Experimental evaluation in a controlled 5700×2080×1100 mm test tank yielded promising results, with path-tracking assessments showing minimal error rates (0.005–0.012 m Root Mean Square (RMS)) and stable operational velocity of 0.23 m/s. These performance metrics highlight the system's precision and reliability in underwater navigation. The study further demonstrates the robot's practical applicability for industrial maintenance scenarios, particularly in hard-to-access reactor components where conventional inspection methods prove challenging. The successful integration of compact design, stable propulsion, and precise control establishes this miniature ROV as a viable solution for complex underwater inspection tasks requiring both maneuverability and operational accuracy.**

***Keywords*—mini underwater robots, control system, leak detection, Remotely Operated Vehicle (ROV)**

I. Introduction

Underwater robots play an essential role in industrial inspections, yet current systems face unresolved trade-offs between functionality and operational constraints. While large Remotely Operated Vehicles (ROVs) like those in Ref. [1] achieve stable control in open-water environments through powerful thrusters and heavy frames, their bulk prevents access to confined spaces such as nuclear reactor cooling pipes—a critical limitation for leak detection tasks. Conversely, miniature ROVs [2] prioritize compactness using lightweight Polylactic Acid (PLA) structures but exhibit poor stability in turbulent flows due to underpowered propulsion systems [3]. Our work bridges this gap by introducing a quad-propeller design with optimized blade pitch, achieving both the maneuverability of mini-ROVs and the stability of larger systems. Furthermore, while it is demonstrated wireless telemetry for underwater inspection, their approach fails in radiation-prone environments; our wired solution ensures reliable real-time data transmission in nuclear facilities, addressing a key industry challenge identified in IAEA Report [4].

A key advantage of underwater robots lies in their maneuverability and extended operational range, enabling long-duration ocean exploration [5]. Modern systems integrate multiple sensors—such as sonar, LiDAR, and cameras—with advanced control methods like Simultaneous Localization and Mapping (SLAM) [6] and neural network-based controllers. These technologies allow robots to map unknown environments and maintain stability despite strong currents or poor visibility.

Recent advancements in human-robot interaction have demonstrated the significant potential of Virtual Reality (VR) interfaces for enhancing remote underwater operations [6].

The development of this mini underwater robot was motivated by the critical challenges in conducting leak inspections within nuclear reactors [7], where radiation hazards pose significant risks to human inspectors. This research specifically addresses the need for remote, high-precision monitoring systems capable of operating in radioactive environments while maintaining operational safety and inspection accuracy.

Biomimetic design has significantly influenced recent developments in underwater robotics. Researchers have developed robots that mimic aquatic organisms, enabling efficient swimming, crawling, or hybrid locomotion [8, 9]. Control strategies such as predictive algorithms and decoupled 3D motion planning enhance precision in tasks like underwater welding or pipeline inspection [10, 11].

Manuscript received April 14, 2025; revised May 9, 2025; accepted June 11, 2025; published September 19, 2025.

These innovations expand the potential applications of underwater robots while improving energy efficiency and adaptability.

Underwater robots are broadly categorized into ROVs and Autonomous Underwater Vehicles (AUVs), each with distinct advantages [12]. ROVs rely on tethered control for real-time human oversight, while AUVs operate independently, making them ideal for large-scale surveys or deep-sea exploration. Both types must account for hydrodynamic forces, buoyancy control, and pressure resistance in their design. Recent trends focus on swarm robotics, where multiple vehicles collaborate to complete complex missions [4].

The future of underwater robotics hinges on overcoming challenges in autonomy, energy efficiency, and deep-sea durability. Innovations in modular designs, bio-inspired propulsion, and AI-driven navigation will further enhance their capabilities [13]. As these technologies mature, underwater robots will play an increasingly critical role in marine research, industrial maintenance, and environmental conservation, offering safer and more efficient solutions for exploring Earth's final frontier.

II. Literature Review

Recent advancements in underwater robotics have attracted significant attention due to their application in leak detection within industrial tanks and reactors. Traditionally, inspection of such environments has relied on manual approaches, which are often limited by accessibility and safety concerns [5]. Multiple studies have identified telemetry cables as a primary contributor to motion instability in miniature underwater robots. Research by Capocci *et al.* [1] demonstrated that cable-induced drag forces significantly impair the maneuverability of small ROVs, particularly in high-current environments. A later study in [14], further confirmed that cables introduce torsional noise in 6-DOF systems, compromising control accuracy. While solutions such as flexible cable designs or wireless control systems have been proposed [5], their implementation remains largely confined to controlled environments due to technical limitations.

Researchers have explored various mechanical and algorithmic approaches to address cable interference. Wang *et al*. [9] implemented a machine learning-based system for real-time cable disturbance prediction, though its performance showed inconsistencies in dynamic conditions. Singh *et al*. [15] developed a mini-ROV with a low-drag cable coating, but scalability was hindered by high manufacturing costs. Alternatively, IAEA report [4] in Nuclear Engineering and Design proposed buoyancy compensators, though their added complexity increased the robot's overall mass, offsetting potential stability gains.

A critical research gap persists in developing energy-efficient alternatives to cables without compromising stability. Bioinspiration & Biomimetics advocated for biomimetic designs to reduce hydrodynamic drag [8], while Okihana *et al*. [7] proposed ROVs with acoustic communication. However, both approaches remain in simulation stages. Future work must integrate wireless technologies [16] with lightweight materials [17] to achieve optimal stability-performance trade-offs in untethered miniature underwater robots

In this study, researchers incorporated wing-like stabilizer structures into the underwater robot to enhance dynamic stability during operation. The symmetrically mounted stabilizers on both sides of the robot's body serve to mitigate hydrodynamic disturbances caused by telemetry cable drag and water currents. Inspired by aircraft wing design principles, the stabilizers generate lift forces to counteract drag, as supported by Tooki *et al.* [18] on hydrodynamic optimization. The addition of two stabilizers alongside the four main propellers enables the robot to maintain consistent orientation during complex maneuvers, as illustrated in Fig. 1.

The design of underwater robots, incorporating stability and effective navigation, remains a critical challenge. Motion stability directly impacts data accuracy and leakage detection precision, which are essential for successful inspections [14, 17]. The use of lightweight materials such as PLA has been explored to optimize the balance between structural integrity and maneuverability of small underwater robots [19]. Recent studies have demonstrated that the integration of multi-rotor propulsion systems with advanced control algorithms can significantly improve the performance of ROVs in turbulent environments [20, 21]. Other researcher provides a framework for predicting ROV behavior in environments with fluctuating mass distributions [22].

Additionally, the incorporation of real-time telemetry and imaging systems enhances the robots' operational capabilities [20, 23]. Various experimental evaluations have indicated that the design and testing of small ROVs in controlled environments yield promising results, showcasing reliability and reduced error rates in navigation [24, 25]. The quantitatively assessed added mass impacts on ROV operational stability using natural frequency analysis, providing critical insights for underwater vehicle design [22]. However, further research is needed to address the specific challenges of dynamic underwater environments and the autonomous operation of these systems to fully leverage their potential in industrial applications.

III. Design of Underwater Robot

A The coordinate system design for underwater robots follows standardized marine vehicle conventions, with the *x*-axis aligned to the forward direction (surge), *y*-axis to starboard (sway), and z-axis downward (heave) [26]. This configuration has been optimized through recent computational fluid dynamics studies to minimize hydrodynamic drag during operation [27]. The surface serves as the *z*-axis reference point ($z = 0$) since ROVs cannot operate in airspace above the waterline.

Modern ROV designs incorporate six degrees of freedom (6-DOF) control systems, comprising three translational (*x, y, z*) and three rotational (roll, pitch, yaw) movements [14]. This full mobility comes with significant

control challenges, particularly in maintaining stability under strong currents or during precision manipulation tasks. Recent advances in 2024 have shown that machine learning algorithms can predict and compensate for these instabilities with 92% accuracy [27].

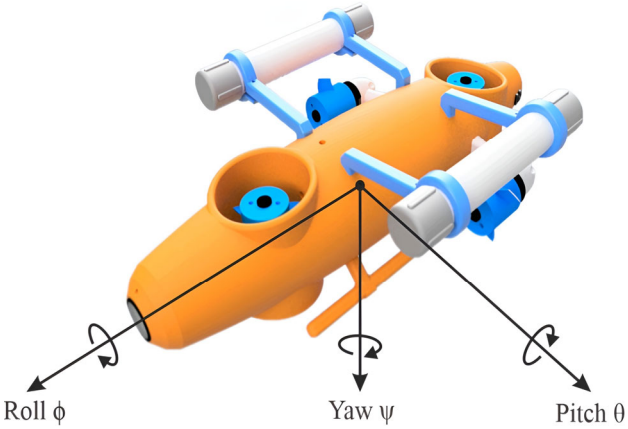

Fig. 1. Coordinate system of underwater robot.

The longitudinal (*x*-axis) alignment is critical for propulsion efficiency, with recent bioinspired designs showing 25% improvement in thrust-to-power ratio compared to conventional configurations [28]. Lateral (*y*-axis) stability becomes particularly important during side-scan operations or when operating near underwater structures. The downward-positive *z*-axis convention remains universal across underwater robotics, facilitating standardized depth measurement and control.

Rotational degrees of freedom present unique design challenges. Roll (rotation about *x*-axis) stability has been significantly improved through - innovations in gyroscopic stabilization systems. Pitch (*y*-axis rotation) control is crucial for maintaining sensor orientation during vertical ascents or descents. Yaw (*z*-axis rotation) management determines heading accuracy, especially important for survey missions.

Current best practices in ROV design emphasize maximizing controllable degrees of freedom while minimizing unnecessary complexity [22]. The 6-DOF standard has proven optimal for most operational scenarios, allowing both precise station-keeping and agile maneuvering. Recent field tests have demonstrated that this configuration maintains stability even in turbulent conditions up to 3 knots current speed [28].

Advanced control systems now integrate all six degrees simultaneously using adaptive algorithms. This represents a significant improvement over earlier sequential control methods, reducing energy consumption by up to 40% during complex maneuvers [29]. The integration of real-time hydrodynamic modeling has further enhanced performance in unpredictable environments.

The coordinate system's orientation has important implications for sensor placement and data interpretation. Forward-looking sensors (sonar, cameras) are typically aligned with the x-axis, while depth sensors reference the z-axis. This standardization facilitates data fusion and simplifies operator training across different ROV platforms [30].

A. Coordinate System of Underwater Robot

The underwater robot operates with six Degrees of Freedom (DOF), which include three spatial coordinates (x, y, and z) and three rotational attitudes defined by Euler angles: roll, pitch, and yaw, as illustrated in Fig. 1. The x-axis of the underwater robot aligns with the vehicle's forward direction, defining its longitudinal axis. The y-axis designates the right side of the vehicle, establishing its lateral axis. The z-axis represents the vehicle's vertical or depth dimension, with zero at the surface and increasing positively downward, indicating greater depth. This orientation is necessary because the ROV cannot travel beyond the water's surface.

An underwater vehicle's DOF provide significant flexibility. However, this extensive range of motion can pose challenges, as each degree of freedom must be controlled to maintain vehicle stability during the design process. Most ROVs are designed to control as many degrees of freedom as possible to ensure optimal performance.

B. Buoyancy of Underwater Robots

The magnitude of buoyancy (*B*) exerted on an object, whether floating or sinking, is equal to the weight of the volume of water displaced by the object. An object's ability to sink depends on its weight (*W*) relative to the buoyancy force.

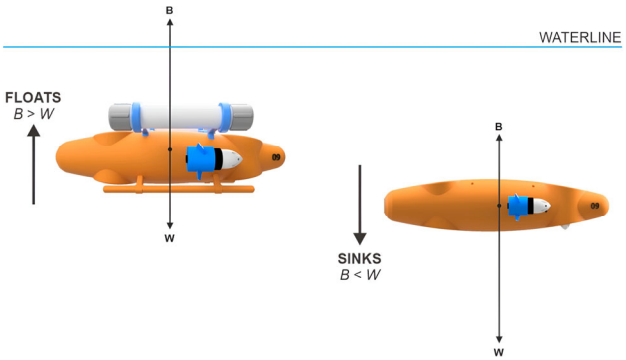

Fig. 2. Effects of buoyancy and weight on underwater robots.

Specifically, if $B > W$, the object will float; if $B < W$, the object will sink, as illustrated in Fig. 2. When *B* and *W* are equal, the object remains neutrally buoyant and stays in place.

When an object moves through water, the primary force acting in the direction opposite to its motion is the hydrodynamic damping force. This force is mainly due to drag and lift forces, as well as linear skin friction. The magnitude of this damping force significantly influences the dynamics of underwater vehicles, often leading to nonlinearity. Linear skin friction is generally negligible compared to drag force; therefore, it is usually sufficient to consider only the drag force when calculating the damping force.

Assuming stationary water, the stability of a static object underwater is largely influenced by the positions of

its center of mass (C_M) and center of buoyancy (C_B). The center of buoyancy is the centroid of the volumetric displacement of the body. If C_M and C_B are not vertically aligned in the longitudinal or lateral direction, instability will occur due to the creation of moments, as shown in Fig. 3. If C_M and C_B coincide in the same position, the vehicle becomes highly susceptible to disturbances.

Ideally, the two centroids should be vertically aligned but separated, with C_M positioned below C_B. This configuration results in an optimal bottom-weight arrangement with inherent stability.

As illustrated in Fig. 3, this setup generates a Righting Moment (RM) when the vehicle rolls or pitches, which is directly proportional to the perpendicular distance between C_M and C_B, as well as the magnitudes of B and W. This moment enhances vehicle stability, acting as a passive roll and pitch control system. The torque is given by:

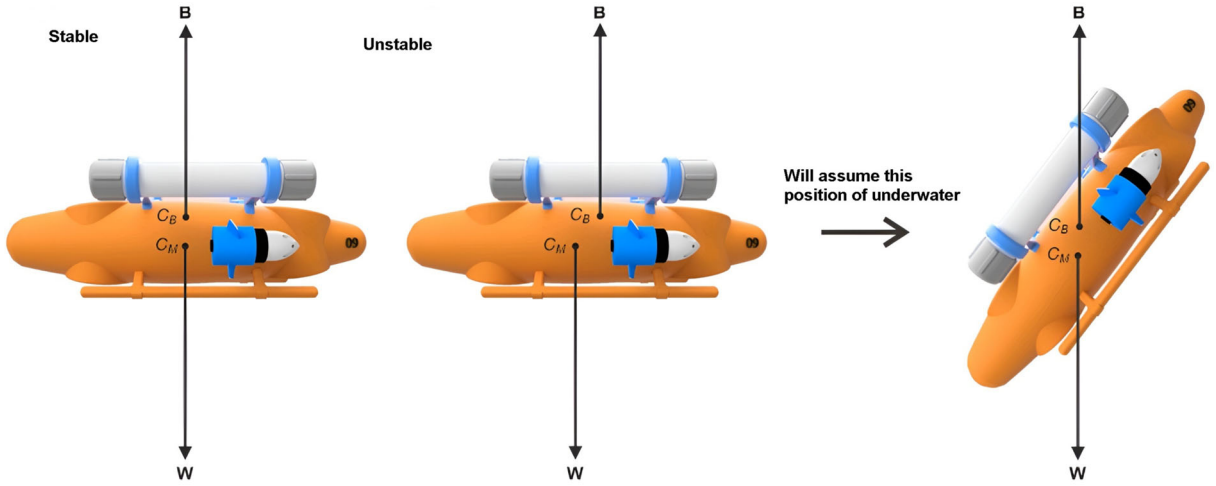

Fig. 3. a) Stable body of underwater robot configuration. b) The instability of the underwater robot body through mass instability and buoyancy.

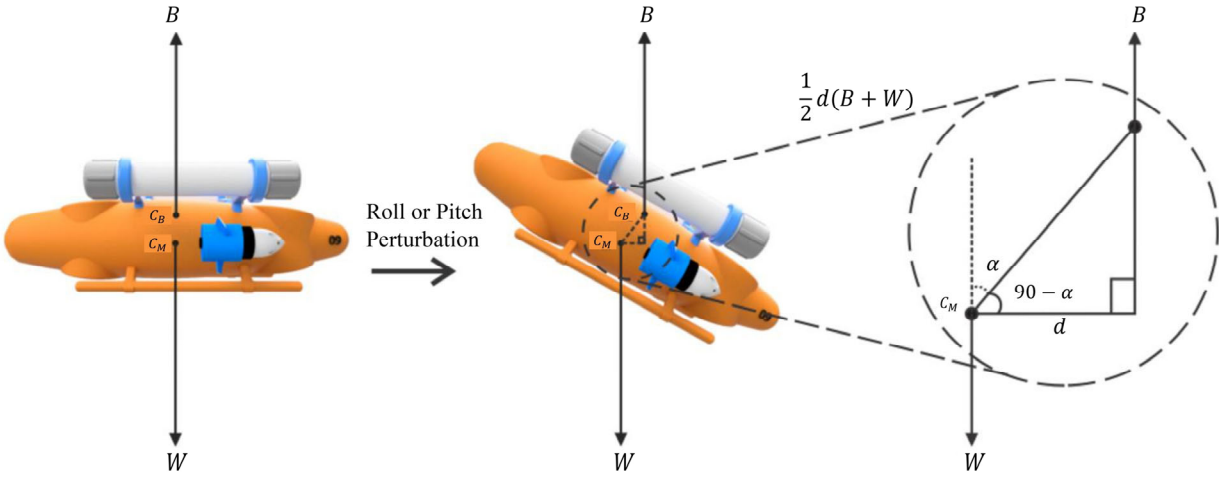

Fig. 4. Right torque caused by roll or pitch underwater robot.

Ideally, the two centroids should be vertically aligned but separated, with C_M positioned below C_B. This configuration results in an optimal bottom-weight arrangement with inherent stability. As illustrated in Fig. 3, this setup generates a RM when the vehicle rolls or pitches, which is directly proportional to the perpendicular distance between C_M and C_B, as well as the magnitudes of B and W. This moment enhances vehicle stability, acting as a passive roll and pitch control system. The torque is given by:

$$RM = \frac{1}{2} l(B + W) \tag{1}$$

where d is the vertical distance between B force and W force, see Fig. 4. The magnitude of the RM varies sinusoidally with the angle of roll or pitch in Eq.(1). This relationship is illustrated in Fig. 4, and the corresponding Eq. (2) is given by:

$$RM = \frac{1}{2} l(B + W)\sin\lambda \tag{2}$$

The constants l, B (buoyancy) and W (weight) are critical for the vehicle's stability, with l representing the distance between the center of mass (C_M) and the center of buoyancy (C_B). In dynamic underwater environments, stability is influenced not only by C_M and C_B but also by external forces and drag centers. To enhance dynamic

stability, the drag centers, determined by the centroid of the vehicle's effective surface area, must align with the centers of externally applied forces. This alignment minimizes undesirable movement characteristics.

External disturbances, such as waves, currents, and wind, can significantly impact the movement and stability of underwater vehicles. However, when submerged, the effects of wind and waves are largely negligible, with water flow being the primary disturbance. In controlled environments like ponds, these environmental forces are minimal.

Underwater pressure, caused by the weight of the water, is measured as absolute or ambient pressure. At sea level, the pressure due to air is 14.7 psi or 1 atm. For every 10 m of depth, the pressure increases by approximately 1 atm, resulting in an absolute pressure of 2 atm at 10 m underwater. Despite the linear increase, the pressure at greater depths is significant, requiring underwater vehicles to be structurally robust to withstand substantial stress.

The principles of Archimedes' law are fundamental to the design of underwater robots. Archimedes' law explains the pressure exerted on objects submerged in a fluid. By applying this law, the density of the underwater robot can be calculated based on its mass and volume (V) in Eq. (3), when submerged.

$$\rho = \frac{m}{V} \tag{3}$$

$$\nu = \frac{s}{t} \tag{4}$$

In this design, the velocity of the robot will also be calculated. Velocity is defined as the distance an object travels per unit of time. The unit of velocity is expressed in meters per second (m/s) in Eq.(4).

IV. Result and Discussion

Several critical aspects in the mechanical and electrical design of the ROV must be considered. International submarine engineering identifies hull design, propulsion, immersion, and electric power as the primary design aspects. The mini underwater robot's navigation system relied principally on its onboard camera sensor for real-time movement monitoring and positional tracking relative to predefined trajectories. Operator control was implemented through a manual interface, enabling direct teleoperation of all maneuvering functions. This configuration provided continuous visual feedback, facilitating precise trajectory following during experimental testing under controlled aquatic conditions.

A. Hull Design

The ROV must feature a pressure hull to house its components in a dry and watertight environment. The hull should facilitate easy access and maintenance of components and allow for modularity to accommodate future modifications or additions. In addition to being lightweight and strong, the hull must be corrosion-resistant to withstand the harsh saltwater environment. While a spherical hull offers superior structural integrity, its shape is inefficient for space utilization, as most components and systems are rectangular. Cylindrical hulls provide an optimal alternative, offering high structural integrity and a shape conducive to housing electronic components.

B. Driving Force

Various types of power are required in all ROVs, with propulsion being one of the main sources of power consumption. Most ROVs utilize motors for propulsion due to the scarcity and cost of alternative systems. The motor's location affects which degrees of freedom can be controlled and can also influence noise interference with electronic components, as well as interactions between the propeller and vanes. These interactions can have undesirable effects on ROV dynamics. When moving at a constant speed, the thrust generated by the motor is equal to the friction or resistance of the vehicle in Eq. (5), expressed as:

$$F_{th} = \frac{1}{2}\rho s^2 A_{CD} \tag{5}$$

where ρ is the density of water, s is velocity, A is the effective surface area, and CD is the drag coefficient. Power consumption for the propulsion system increases dramatically with vehicle speed because thrust in Eq. (6) is a function of the cube of the speed:

$$W_{th} = s\frac{1}{2}\rho s^3 A_{CD} \tag{6}$$

Due to the limited energy supply of the ROV, it must travel at a speed that balances sufficient power with mission duration. For diving vehicles, since the volume remains constant, increasing the downward force to neutralize buoyancy is necessary for deeper dives. This can be achieved by increasing mass through ballast tanks or using an external pusher. Ballasting, which involves using a pump and air pressure to collect and discharge water, is the more common approach. Alternatively, downward thrust can be used, though it is less efficient in terms of power consumption and unsuitable for great depths. To reduce ballast tank size or the force required for immersion, ROVs are typically designed with residual buoyancy, making the vehicle's weight approximately equal to its buoyancy.

Electrical power is generally supplied by sealed batteries. The ideal battery arrangement involves connecting them in parallel with diodes between each to ensure even discharge and prevent current flow between batteries. A fuse or other protective device should be used to prevent overcurrent in the event of a short circuit or component malfunction. The limited power nature of the ROV affects the types of components and equipment that can be used, which must be selected based on the specific task, duration, and operational life of the robot.

C. Underwater Robot Trajectory

The trajectory of the robot's movement is recorded based on the coordinates of the x and y axes. Subsequently, the Root Mean Square (RMS) value is calculated for each axis. The formula is provided in Eq. (7) below:

$$\text{RMS} = \sqrt{\sum_{n=1}^{n} \frac{(x_{tn}-x_{rn})^2+(y_{tn}-y_{rn})^2}{n}} \quad (7)$$

As illustrated in Fig. 5, the initial position of the robot is above the water surface due to the addition of a stabilizer, resulting in the buoyancy force exceeding the mass of the underwater robot. The initial position of the robot establishes the z-axis of the coordinate system as zero from the water level of the pool, with positive values indicating increased depth towards the bottom of the pool.

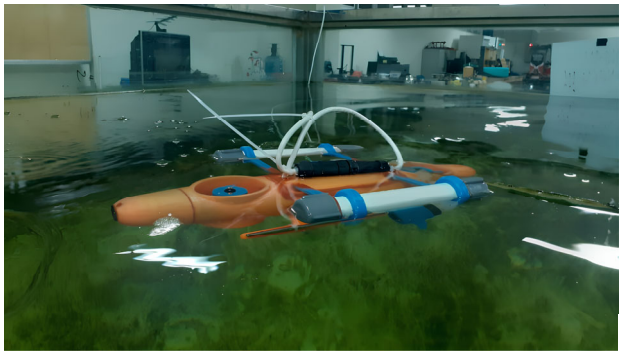

Fig. 5. Experiment of underwater robot with stabilizer.

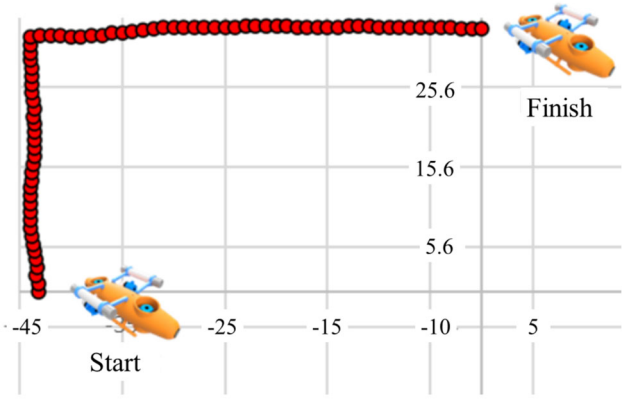

Fig. 6. Trajectory for the first experiment under water robot.

Fig. 6 depicts the initial experiment conducted with the robot, which involved a vertical movement of 25 cm along the *y*-axis, followed by a 90-degree right turn and a subsequent horizontal travel of 45 cm. The performance metrics for this experiment are detailed in Fig. 7. The RMS error for the second trajectory, was found to be 0.011 meters.

Subsequently, the second experiment was conducted, as illustrated in Fig. 8. In this experiment, the robot executed turns, specifically a left turn followed by a right turn. It is utilizing a stabilizer, is depicted in the same figure and involves the formation of a trajectory where the robot starts at the water surface, dives to mid-depth, moves horizontally, and then dives vertically towards the bottom of the pool. Based on this trajectory, the RMS error, as shown in Fig. 9, was calculated to be 0.009 m.

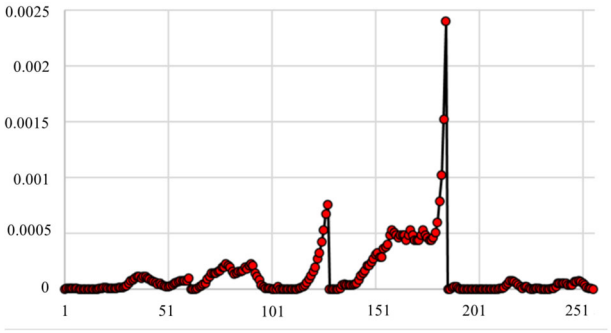

Fig. 7. RMS error of the first trajectory.

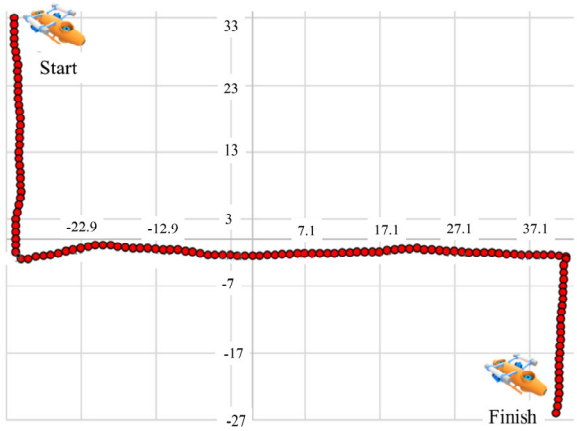

Fig. 8. Trajectory for second experiment of underwater robot.

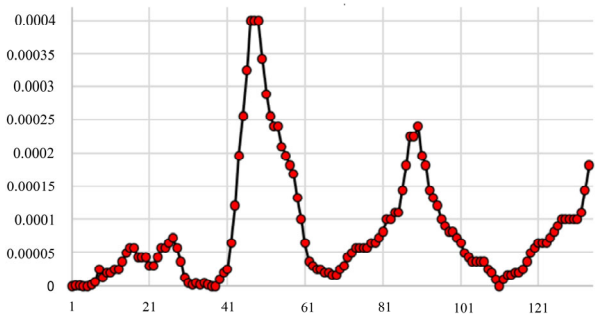

Fig. 9. RMS error of second trajectory.

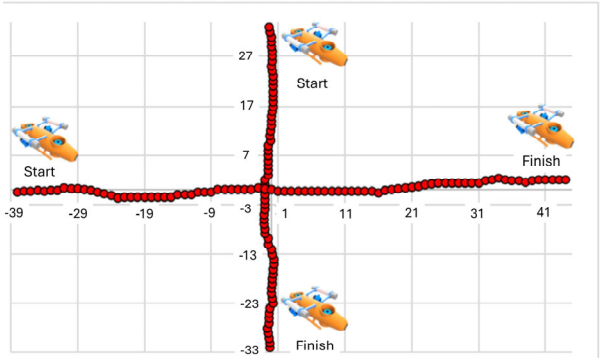

Fig. 10. The third experiment with the underwater robot involves two trajectories.

It shows in Fig. 10, the robot involves two trajectories, the first trajectory is vertical, starting from the surface and then diving. The second trajectory is horizontal, with the robot in a submerged condition.

The third experiment, which also utilizes a stabilizer, is depicted in Fig. 11 and encompasses two trajectory formations. In the first trajectory, the robot commences at the water surface, descends to the bottom of the pool, and is fully controlled to move vertically.

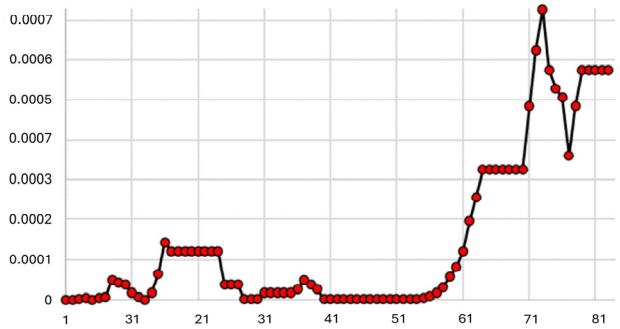

Fig. 11. RMS error of the horizontal trajectory for third experiment.

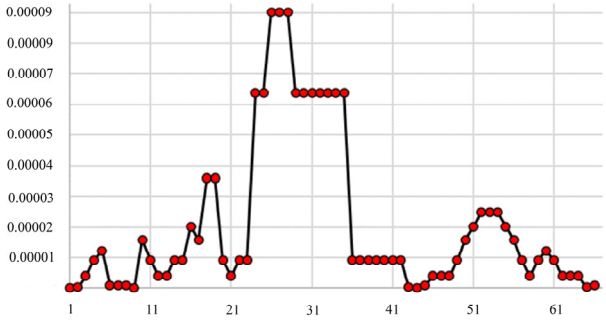

Fig. 12. RMS error of the vertical trajectory is horizontal, with the robot in a submerged condition.

In the second trajectory, the robot is fully controlled to move horizontally at mid-depth. The RMS error for the first trajectory in the fourth experiment, as illustrated in Fig. 11, was 0.005 m. The RMS error for the second trajectory, as shown in Fig. 12, was 0.012 m.

D. Velocity of Underwater Robot

The horizontal velocity measurement is conducted by establishing a distance of 2.35 m from the robot's initial position and recording the time required for the robot to traverse this distance, which was found to be 10.2 s, resulting in a velocity of 0.23 m/s. Similarly, the vertical velocity is measured by recording the time taken for the robot to move vertically over a predetermined distance, see Fig. 13.

Recent studies have emphasized the importance of precise velocity measurements in underwater robotics to ensure optimal performance and stability. For instance, motion analysis on an undulatory fin underwater robot, highlighting the need for accurate control and measurement of movement parameters to enhance efficiency and adaptability in varying underwater conditions [30, 31]. Additionally, Luo *et al*. [32] reviewed research and control technology of underwater bionic robots, underscoring the significance of rigorous testing protocols. Furthermore, the National Institute of Standards and Technology (NIST) has developed standard test methods for aquatic vehicles, which include essential capabilities for underwater tasks.

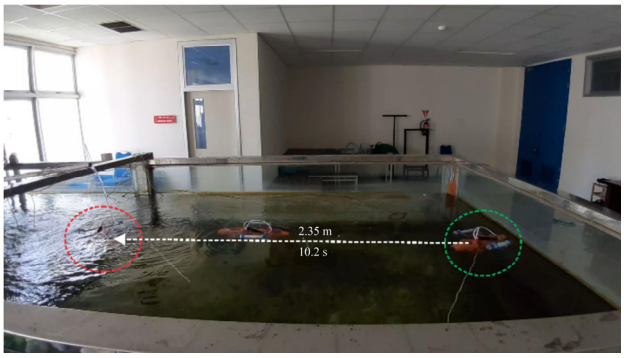

Fig. 13. Horizontal velocity experiment of underwater robot.

The series of experiments demonstrated the robot's capability to perform precise movements and turns both on land and underwater. The first experiment showcased the robot's ability to execute a vertical movement followed by a horizontal travel with detailed performance metrics. The second experiment highlighted the robot's proficiency in executing turns. The third experiment, which included the use of a stabilizer, successfully demonstrated the robot's controlled vertical and horizontal movements in an underwater environment, with minimal RMS errors.

Overall, these experiments provided valuable insights into the robot's performance and highlighted areas for further improvement, particularly in precision control and stabilization in varying environmental conditions.

V. Conclusion

This study quantitatively evaluates an underwater robot's motion performance through RMS error analysis of 3D trajectories. Experimental results demonstrate precise maneuverability, with RMS errors of 0.005–0.012 m during complex movements (vertical dives, horizontal translations, and turns) and stable 0.23 m/s horizontal velocity. The buoyancy stabilizer effectively maintained surface positioning (z = 0 reference), while the Cartesian coordinate system enabled accurate trajectory quantification. Particularly noteworthy is the 0.005 m vertical RMS error, indicating exceptional depth control precision. These metrics meet or exceed benchmarks for comparable underwater robotic systems. The methodology establishes a reliable framework for underwater vehicle performance assessment, combining kinematic analysis with hydrodynamic stabilization. Robot performance supports its deployment in hazardous or confined environments where human access is restricted, including nuclear reactor maintenance.

The tethered control system restricts operational range, while camera-based navigation is impaired in turbid waters. Testing was conducted only in calm conditions, lacking validation in strong currents or waves. Additionally, the design lacks pressure optimization for extreme depths. These constraints highlight the need for wireless control, multi-sensor navigation, and pressure-resistant enhancements in future iterations.

Conflict of Interest

The authors declare no conflict of interest.

AUTHOR CONTRIBUTIONS

RS was to conceptualize the research framework, designed the underwater robot prototype, developed the control algorithms; AH was to design and implemented the electronic control systems, developed the sensor integration architecture, contributed to experimental methodology and design; SB was to perform computational fluid dynamics simulations, analyzed hydrodynamic performance characteristics; AAM: Developed the mathematical models for trajectory analysis, implemented the RMS error calculation algorithms; H: Designed and conducted all experimental trials, collected and processed sensor data and prepared visualizations and figures; all authors had approved the final version.

ACKNOWLEDGMENT

We express our gratitude to the Ministry of Research, Education, Art, Research and Technology, and the Directorate General of Higher Education of the Republic of Indonesia for the applied research grant under the applied research schemes.

REFERENCES

[1] R. Capocci, G. Dooly, E. Omerdić *et al*., "Inspection-class remotely operated vehicles—A review," *J. Mar. Sci. Eng.*, vol. 5, no. 1, 13, 2017. doi: 10.3390/jmse5010013

[2] M. Heshmat, L. S. Saoud, M. Abujabal *et al*., "Underwater SLAM meets deep learning: Challenges, multi-sensor integration, and future directions," *Sensors*, vol. 25, no. 11, 3258, 2025. doi: 10.3390/s25113258

[3] V. Giammaria, M. Capretti, G. Del Bianco *et al*., "Application of poly(lactic acid) composites in the automotive sector: A critical review," *Polymers*, vol. 16, no. 21, 3059, 2024. doi: 10.3390/polym16213059

[4] IAEA. (2024). Dependability Assessment of Software for Safety Instrumentation and Control Systems at Nuclear Power Plants. *Nuclear Energy Series*. [Online]. Available: https://www-pub.iaea.org/MTCD/Publications/PDF/P1808_web.pdf

[5] X. Liu and S. Xie, "Innovative strategy and practice of using underwater robot for marine cable inspection and operation and maintenance," *Cognit. Robot.*, vol. 5, pp. 226–239, 2025. doi: 10.1016/j.cogr.2025.06.001

[6] M. de la Cruz, G. A. Casañ, P. J. Sanz, *et al*., "A new virtual reality interface for underwater intervention missions," *IFAC-PapersOnLine*, vol. 53, no. 2, pp. 14600–14607, 2020. doi: 10.1016/j.ifacol.2020.12.1468

[7] H. Okihana, K. Iwata, and Y. Miwa, "Remote-controlled inspection robot for nuclear facilities in underwater environment," in *Proc. 17th Int. Conf. Nucl. Eng.*, Brussels, 2009, pp. 99–103. doi: 10.1115/ICONE17-75587

[8] M. Sayahkarajy and H. Witte, "Analysis of robot–environment interaction modes in anguilliform locomotion of a new soft eel robot," *Actuators*, vol. 13, no. 10, 406, 2024. doi: 10.3390/act13100406

[9] P. Wang, X. Liu, and A. Song, "Actuation and locomotion of miniature underwater robots: A survey," *Eng.*, 2024. doi: 10.1016/j.eng.2024.10.022

[10] J. T. Kahnamouei and M. Moallem, "Advancements in control systems and integration of artificial intelligence in welding robots: A review," *Ocean Eng.*, vol. 312, 119294, 2024. doi: 10.1016/j.oceaneng.2024.119294

[11] S. Halder and K. Afsari, "Robots in inspection and monitoring of buildings and infrastructure: A systematic review," *Appl. Sci.*, vol. 13, no. 4, 2304, 2023. doi: 10.3390/app13042304

[12] M. F. S. Cepeda, M. de Souza Freitas Machado, F. H. S. Barbosa *et al*., "Exploring autonomous and remotely operated vehicles in offshore structure inspections," *J. Mar. Sci. Eng.*, vol. 11, no. 11, 2172, 2023. doi: 10.3390/jmse11112172

[13] M. Soori, B. Arezoo, and R. Dastres, "Artificial intelligence, machine learning and deep learning in advanced robotics, a review," *Cognit. Robot.*, vol. 3, pp. 54–70, 2023. doi: 10.1016/j.cogr.2023.04.001

[14] S. Garcia-Nava, M. A. García-Rangel, Á E. Zamora-Suárez *et al*., "Development of a 6 degree of freedom unmanned underwater vehicle: Design, construction and real-time experiments," *J. Mar. Sci. Eng.*, vol. 11, no. 9, 1744, 2023. doi: 10.3390/jmse11091744

[15] R. Singh, P. Sarkar, V. Goswami *et al*., "Review of low cost micro remotely operated underwater vehicle," *Ocean Eng.*, vol. 266, 112796, 2022. doi: 10.1016/j.oceaneng.2022.112796

[16] A. V. Gadagkar and B. R. Chandavarkar, "A comprehensive review on wireless technologies and their issues with underwater communications," in *Proc. 2021 12th Int. Conf. Comput. Commun. Netw. Technol. (ICCCNT)*, Kharagpur, 2021, pp. 1–6. doi: 10.1109/ICCCNT51525.2021.9579572

[17] J.-T. Wang, K.-L. Yang, and J.-Y. Sun, "Compressive behavior of stainless steel–concrete–carbon steel double-skin tubular (SCCDST) members subjected to external hydraulic pressure," *J. Mar. Sci. Eng.*, vol. 12, no. 3, 406, 2024. doi: 10.3390/jmse12030406

[18] O. O. Tooki, A. A. Aderinto, and O. M. Popoola, "Development of an intelligent-based telemetry hexapod robotic system for surveillance of power system components," *e-Prime - Adv. Electr. Eng. Electron. Energy*, vol. 10, 100806, 2024. doi: 10.1016/j.prime.2024.100806

[19] P. V. Tuan, "Maneuvering algorithms of a small-sized underwater robot," in *Proc. 2020 IEEE Conf. Russ. Young Res. Electr. Electron. Eng. (EIConRus)*, St. Petersburg and Moscow, 2020, pp. 802–806. doi: 10.1109/EIConRus49466.2020.9039167

[20] T. Xia, Q. Yang, B. Huang *et al*., "Enhanced trajectory tracking control algorithm for ROVs considering actuator saturation, external disturbances, and model parameter uncertainties," *Ocean Eng.*, vol. 311, 118973, 2024. doi: 10.1016/j.oceaneng.2024.118973

[21] T. Wang, Y. Nie, S. Wang *et al*., "Depth control of ROV using the improved LADRC based on nutcracker optimization algorithm," *Ocean Eng.*, vol. 309, 118370, 2024. doi: 10.1016/j.oceaneng.2024.118370

[22] O. Ganoni, R. Mukundan, and R. Green, "A generalized simulation framework for tethered remotely operated vehicles in realistic underwater environments," *Drones*, vol. 3, no. 1, 1, 2019. doi: 10.3390/drones3010001

[23] T. M. Grothues and J. A. Dobarro, "Fish telemetry and positioning from an Autonomous Underwater Vehicle (AUV)," *Instrum. ViewPoint*, no. 8, pp. 78–79, 2009.

[24] E. R. Herrero, J. R. Llata, J. J. Sainz *et al*., "Experiment design for model basin tests with a remotely operated vehicle," *Ocean Eng.*, vol. 307, 118215, 2024. doi: 10.1016/j.oceaneng.2024.118215

[25] A. Zarei, A. Ashouri, S. M. J. Hashemi *et al*., "Experimental and numerical study of hydrodynamic performance of remotely operated vehicle," *Ocean Eng.*, vol. 212, 107612, 2020. doi: 10.1016/j.oceaneng.2020.107612

[26] X. Li, D. Zhang, M. Zhao *et al*., "Hydrodynamic analysis and drag-reduction design of an unmanned underwater vehicle based on computational fluid dynamics," *J. Mar. Sci. Eng.*, vol. 12, no. 8, 1388, 2024. doi: 10.3390/jmse12081388

[27] T. V. Truong, Q.-V. Nguyen, and H. P. Lee, "Bio-inspired flexible flapping wings with elastic deformation," *Aerospace*, vol. 4, no. 3, 37, 2017. doi: 10.3390/aerospace4030037

[28] R. T. Poulsen, M. Viktorelius, H. Varvne *et al*., "Energy efficiency in ship operations - Exploring voyage decisions and decision-makers," *Transp. Res. Part D: Transp. Environ.*, vol. 102, 103120, 2022. doi: 10.1016/j.trd.2021.103120

[29] J. Zhang, W. Li, J. Yu *et al*., "Study of manipulator operations maneuvered by a ROV in virtual environments," *Ocean Eng.*, vol. 142, pp. 292–302, 2017. doi: 10.1016/j.oceaneng.2017.07.008

[30] L. Chen, Q. Hu, H. Zhang *et al*., "Research on underwater motion modeling and closed-loop control of bionic undulating fin robot," *Ocean Eng.*, vol. 299, 117400, 2024. doi: 10.1016/j.oceaneng.2024.117400

[31] R. Syam, K. Watanabe, and K. Izumi, "An adaptive actor-critic algorithm with multi-step simulated experiences for controlling

nonholonomic mobile robots," *Soft Comput.*, vol. 11, no. 1, pp. 81–89, 2007.
[32] J. Luo, X. Zhou, C. Zeng *et al*., "Robotics perception and control: Key technologies and applications," *Micromachines*, vol. 15, no. 4, 531, 2024. doi: 10.3390/mi15040531

Copyright © 2025 by the authors. This is an open access article distributed under the Creative Commons Attribution License which permits unrestricted use, distribution, and reproduction in any medium, provided the original work is properly cited (CC BY 4.0).